Anomalous High-Pressure Jahn-Teller Behavior in $CuWO_4$

J. Ruiz-Fuertes,[1,2,*] A. Segura,[1,2] F. Rodríguez,[1,3] D. Errandonea,[1,2] and M. N. Sanz-Ortiz[1,3]

[1]*MALTA Consolider Team*

[2]*Departamento de Física Aplicada—ICMUV, Universitat de València, Edificio de Investigación, c/ Dr. Moliner 50, 46100 Burjassot, Valencia, Spain*

[3]*DCITIMAC, Facultad de Ciencias, Universidad de Cantabria, 39005 Santander, Spain*

(Received 6 February 2012; published 18 April 2012)

High-pressure optical-absorption measurements performed in $CuWO_4$ up to 20 GPa provide experimental evidence of the persistence of the Jahn-Teller (JT) distortion in the whole pressure range both in the low-pressure triclinic and in the high-pressure monoclinic phase. The electron-lattice couplings associated with the $e_g(E \otimes e)$ and $t_{2g}(T \otimes e)$ orbitals of Cu^{2+} in $CuWO_4$ are obtained from correlations between the JT distortion of the CuO_6 octahedron and the associated structure of Cu^{2+} d-electronic levels. This distortion and its associated JT energy (E_{JT}) decrease upon compression in both phases. However, both the distortion and associated E_{JT} increase sharply at the phase-transition pressure ($P_{PT} = 9.9$ GPa), and we estimate that the JT distortion persists for a wide pressure range not being suppressed up to 37 GPa. These results shed light on the transition mechanism of multiferroic $CuWO_4$, suggesting that the pressure-induced structural phase transition is a way to minimize the distortive effects associated with the toughness of the JT distortion.

DOI: 10.1103/PhysRevLett.108.166402 PACS numbers: 71.70.Ej, 61.50.Ks, 62.50.−p, 64.70.kg

Electron-lattice coupling is one of the fundamental issues to understand a wide variety of relevant physical phenomena in materials science [1–6]. In particular, the $E \otimes e$ Jahn-Teller (JT) effect, involving orbitally degenerate e_g electrons and lattice distortions (or vibrations) of e_g symmetry, is known to play a crucial role in many physical phenomena of transition-metal oxides such as colossal magnetoresistance [7], insulator-to-metal transition [8,9], or spin transition phenomena [10,11]. The study of electron-lattice coupling under high-pressure conditions has become a key topic in condensed matter physics [4] since the discovery of the increase of critical temperature in $Ba_2LaCu_3O_{7-y}$ under compression [3]. In general, the knowledge of how electron-lattice couplings and their associated phenomena behave in compound series and under compression has received a lot of attention during the past decade.

In octahedral Cu^{2+} or Mn^{3+} oxides, the JT effect yields low-symmetry distortion around the transition-metal ion increasing the stabilization energy (E_{JT}) [5,10]. Basic models predict the reduction of the JT distortion upon compression due to the hardening of the coupled vibration or the relative weakening of the electron-lattice coupling induced by electron delocalization. Electron-lattice coupling can be eventually suppressed under high-pressure conditions leading to the JT distortion quenching [8–10]. The lack of distortion in the metallic phase of many transition-metal oxides is usually associated with such suppression along with the insulator-to-metal transitions ($LaMnO_3$). The pressure dependences of E_{JT} and JT distortion, $\rho = \sqrt{Q_\theta^2 + Q_\varepsilon^2}$, described in terms of the tetragonal and rhombic normal coordinates $(Q_\theta, Q_\varepsilon)$ for strongly coupled d^4 and d^9 transition-metal systems can be found elsewhere [10–12]. According to estimates based on the volume dependence of electron-lattice coupling and vibrational energy of the coupled mode, it is unlikely that a static $E \otimes e$ JT distortion increases after volume compression along a pressure-induced phase transition. However, recent high-pressure structural studies in $CuWO_4$ found the opposite behavior [13]. We will show how such an unusual behavior is a consequence of the reaction of the CuO_6 octahedron against the JT strength. Electronic and crystal structure correlations performed in this work suggest that the triclinic-to-monoclinic phase transition in $CuWO_4$ is mainly driven by reorientations of the CuO_6 octahedra towards easier-distortion directions as a way to preserve the JT distortion. Thus this system constitutes a model example of a cooperative JT-driven structural phase transition induced by pressure.

Here, we investigate the d-electron structure associated with Cu^{2+} in $CuWO_4$ by high-pressure optical-absorption spectroscopy to establish structural correlations yielding the first experimental electron-lattice coupling determination in Cu^{2+}. We aim to find the relation between E_{JT} and $\rho \approx Q_\theta$ ($Q_\varepsilon \approx 0$), the pressure dependence of which is known from x-ray diffraction (XRD) [13].

$CuWO_4$ crystallizes in a triclinic ($P\bar{1}$) phase at ambient conditions [Fig. 1(a)] and is antiferromagnetic below $T_N = 23$ K. It undergoes a structural phase transition at 10 GPa, to a monoclinic ($P2/c$) wolframite-type structure. The phase transition involves an abrupt reorientation of the CuO_6 octahedra that remain highly distorted in the high-pressure phase.

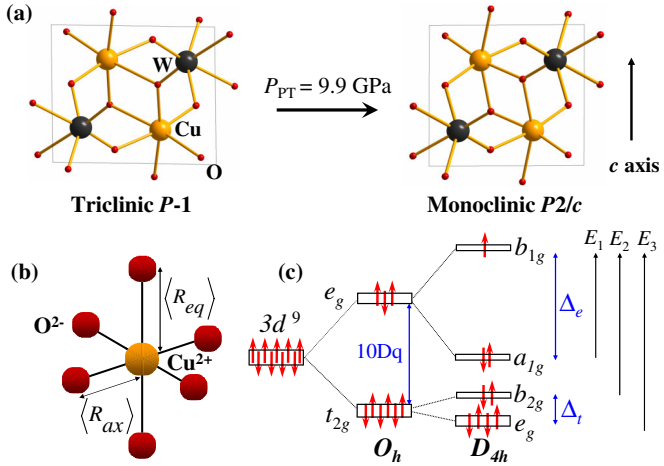

FIG. 1 (color online). (a) Crystal structure of $CuWO_4$ low-pressure triclinic (left) and high-pressure monoclinic (right) phases. (b) CuO_6 octahedral simplified sketch showing the pseudoelongated D_{4h} symmetry. The equatorial distance $\langle R_{eq} \rangle$ corresponds to the average of the four equatorial distances, while the axial distance $\langle R_{ax} \rangle$ is the average of the two axial ones. (c) Correlation diagram of the Cu^{2+} d levels in O_h and D_{4h} symmetries. Arrows indicate the three observed electronic transitions E_1, E_2, and E_3. The tetragonal splitting of the parent octahedral e_g and t_{2g} orbitals is $\Delta_e = E_1$ and $\Delta_t = E_3 - E_2$, respectively.

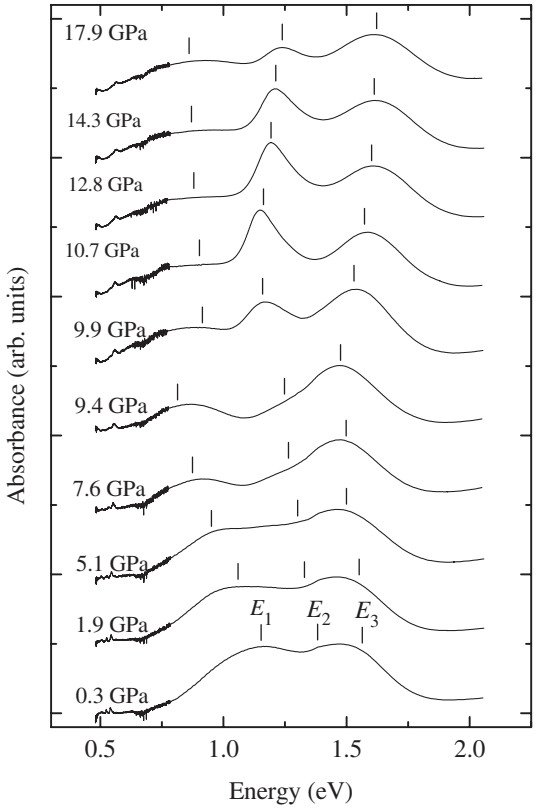

FIG. 2. Variation of the optical-absorption spectrum of $CuWO_4$ with pressure. Ticks show the placement of the three absorption bands.

The variation of the optical-absorption spectrum of $CuWO_4$ with pressure, for both the triclinic and monoclinic phases, is shown in Fig. 2. We used (010) cleavage single crystals with thicknesses from 10 to 20 μm that were loaded together with a ruby chip into a 40 μm-thickness, 250 μm-diameter hydrostatic cavity placed between two 500 μm-culet diamonds of a membrane-type anvil cell. Both methanol-ethanol-water (16:3:1) and silicone oil were used as pressure-transmitting media. The spectroscopy setup is described elsewhere [14,15].

The absorption spectra of $CuWO_4$ (Fig. 2) can be explained on the basis of Cu^{2+} d-d intraconfigurational transitions within a JT-distorted CuO_6 with pseudoelongated D_{4h} coordination [Fig. 1(b)]. The absorption bands basically correspond to electronic transitions from the parent octahedral t_{2g} and e_g filled orbitals e_g, b_{2g}, and a_{1g} to the singly occupied b_{1g} orbital [Fig. 1(c)]. These transitions, which are usually weak in centrosymmetric systems, appear enhanced in $CuWO_4$ by both noncentrosymmetric crystal-field distortions and the exchange mechanism [16]. The two broad bands observed in the low-pressure phase ($P < 9.9$ GPa) correspond to E_1, E_2, and E_3 following the scheme of Fig. 1(c). As usually observed in Cu^{2+} oxides, the two crystal-field transitions associated with the t_{2g}-octahedral orbitals overlap, making their assignment difficult [17]. However, these bands are resolved by polarized absorption spectroscopy (Fig. 3). Because of the distinct band intensity shown by the absorption spectrum in each polarization, we have derived a difference spectrum, which contains only the two higher energy transitions. Hence, we assign $E_1 = 1.16$ eV to $a_{1g} \rightarrow b_{1g}$, $E_2 = 1.34$ eV to $b_{2g} \rightarrow b_{1g}$, and $E_3 = 1.56$ eV to $e_g \rightarrow b_{1g}$ at ambient pressure. The corresponding tetragonal splitting of t_{2g} and e_g octahedral orbitals are $\Delta_e = E_1 = 1.16$ eV and $\Delta_t = E_3 - E_2 = 0.22$ eV. Upon compression, E_1, E_2, and E_3 shift to lower energies up to 9.4 GPa. Accordingly, Δ_e and Δ_t decrease with pressure and correlate with the reduction of the JT distortion observed by x-ray-absorption spectroscopy and XRD [13] (Fig. 4). At $P > 9.9$ GPa, the spectrum abruptly changes, and an additional narrow band appears at 1.19 eV; this change in the electronic structure is due to the pressure-induced triclinic-to-monoclinic phase transition [13,18,19]. According to XRD and x-ray-absorption spectroscopy [13], the Cu^{2+} elongated low-symmetry coordination remains in the high-pressure phase, as it is confirmed by the distinctive d-splitting pattern related to the JT distortion. The magnitude of the pseudotetragonal distortion sharply increases, and the O-Cu-O elongation changes from one direction to another at the phase transition [Fig. 1(a)]. This structural change is also detected by Raman spectroscopy through the abrupt redshift in the Cu-O-related mode at 316 cm^{-1} ($P = 0$ GPa) and the different pressure coefficient found for each phase [19].

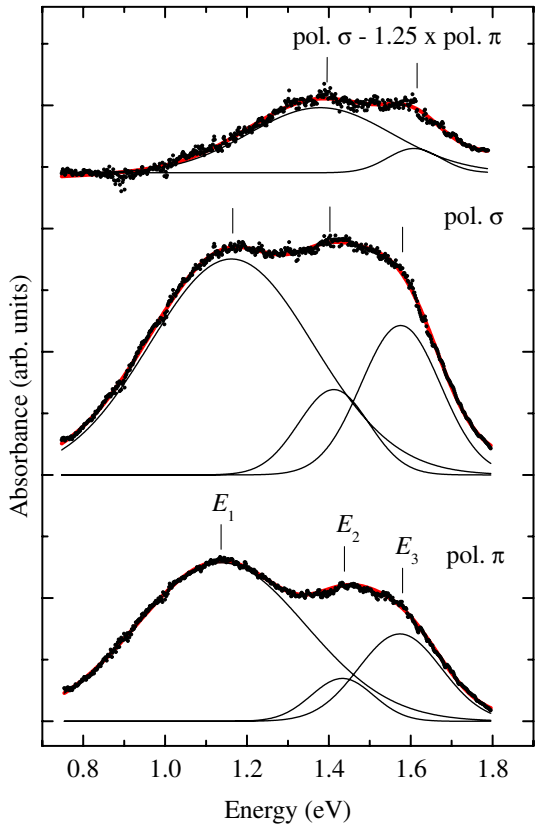

FIG. 3 (color online). Polarized absorption spectrum of $CuWO_4$ along the two extinction directions π and σ in the (100) plane. Each spectrum was obtained at ambient conditions in two polarizations allowing us to resolve the E_2 band. The Gaussian fits to the three electric-dipole crystal-field transitions of Cu^{2+} at ambient pressure (D_{4h} symmetry) are included. The top figure shows the E_1 spectral subtraction to resolve E_2 and E_3.

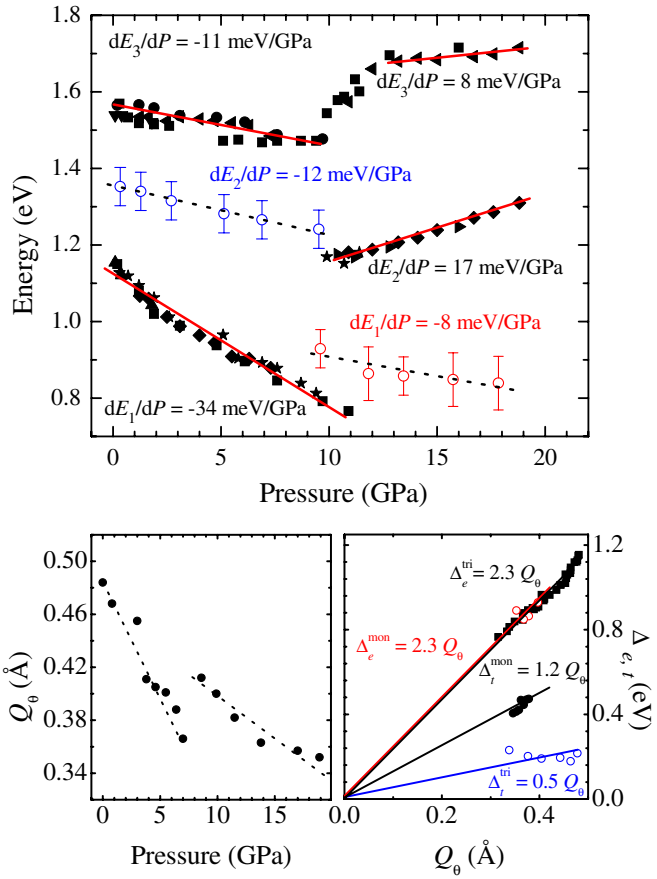

FIG. 4 (color online). Pressure dependence of the transition energy for E_1, E_2, and E_3 (on top). The lines represent least-square fits to the experimental data. The large error bars represent uncertainty due to masking effects. Hollow colored circles represent E_2 (blue) and E_1 (red) at the triclinic and monoclinic phases, respectively. The bottom-left part of the figure shows the variation of the JT distortion Q_θ with pressure [13]. The variations of the e_g- and t_{2g}-orbital splittings Δ_e and Δ_t as a function of the JT distortion Q_θ in the low-pressure-triclinic and high-pressure-monoclinic phases are shown in the bottom-right figure.

Figure 4 shows the variation of E_1, E_2, and E_3 with pressure for the two phases and the corresponding variations of Δ_e and Δ_t as a function of the JT distortion $\rho = Q_\theta$ ($Q_\varepsilon \approx 0$) of the CuO_6 octahedron. In the low-pressure phase, E_3 redshifts at a rate of -11 meV GPa^{-1}, and the masked E_2 shifts -12 meV GPa^{-1}. However E_1 exhibits a pronounced redshift of -34 meV GPa^{-1}, which correlates with the decrease with pressure of the CuO_6 distortion derived from XRD. The sudden increase experienced by all E_1, E_2, E_3, and Q_θ ($Q_\varepsilon \approx 0$) at 9.9 GPa shows the phase-transition onset. In the high-pressure monoclinic phase, E_1 slightly decreases with pressure, but E_2 and E_3 increase in such a way that Δ_e and Δ_t decrease with pressure (increase with Q_θ). These findings are noteworthy, as they provide the dependences of Δ_e and Δ_t with P and Q_θ which are directly related to the electron-lattice coupling through $\partial\Delta_{e,t}/\partial Q_\theta$. In both the low-pressure triclinic and high-pressure monoclinic phases, the e_g splittings depend linearly with Q_θ as $\Delta_e = K_e Q_\theta$, with $K_e = 2.3$ eV $Å^{-1}$. The same dependence is found for $\Delta_t = K_t Q_\theta$, although a different coupling coefficient is measured in each phase: $K_t = 0.5$ and 1.2 eV $Å^{-1}$ for the triclinic and monoclinic phases, respectively. These values are in good agreement with previous structural correlations in Cu^{2+} compound series involving $CuCl_6$ and CuF_6 [11,17], with K_e and K_t values of 2.4 and 0.4 eV $Å^{-1}$, respectively. It must be noted that the electron-lattice coupling coefficient in the JT theory, named A_e in $E \otimes e$ (A_t in $T \otimes e$), is related to the JT splitting derivative as $A_e = 1/2\partial\Delta_e/\partial Q_\theta$ ($A_t = 2/3\partial\Delta_t/\partial Q_\theta$) [20]. In the $E \otimes e$ (or $T \otimes e$) model, A_e (or A_t) and the force constant of the corresponding lattice mode determine the stabilization energy and the corresponding JT distortion of the CuO_6 octahedron [18,20].

Following extended x-ray-absorption fine structure spectroscopy and XRD results [13], we deduce that the axial bond length variation in the low-pressure phase, $\partial R_{ax}/\partial P = -0.016$ Å GPa^{-1}, is an order of magnitude larger than the equatorial one, $\partial R_{eq}/\partial P = -0.002$ Å GPa^{-1}. According

to this, pressure-induced suppression of the JT distortion should occur at about 37 GPa. A similar estimate is obtained by extrapolating structural data from the high-pressure monoclinic phase, thus suggesting that pressure-induced JT quenching towards a regular octahedron is mainly governed by the JT stabilization energy of the CuO_6 rather than the particular crystal phase to which it belongs. In fact, a similar quenching pressure was derived for $CuCl_6$ in Rb_2CuCl_4 [12], where the JT energy $E_{JT} = E_1/4 = 0.3$ eV is similar to the measured in $CuWO_4$. This feature envisages the difficulty to suppress the JT distortion in Cu^{2+} systems, for which severe pressure conditions are required to overpass E_{JT}. The high stability of the CuO_6 distortion, persisting below 37 GPa in $CuWO_4$, forces the axial O-Cu-O to flip direction towards easier-distortion paths as a way to react against compression. This reaccommodation of the CuO_6 octahedron along easy-distortion directions may be considered the origin of the phase transition; we thus suggest that the JT effect is the main driving force triggering the structural transition. This proposed scenario correlates with spectroscopic results. The rapid E_{JT} decrease with pressure in the triclinic phase (-90 meV in 10 GPa) involves an important anisotropy stress along the CuO_6 axial distortion, which is eventually released in the triclinic-to-monoclinic phase transition, as it is reflected by the unexpected increase of Q_θ and E_{JT} observed at the phase-transition pressure (Fig. 4).

In conclusion, optical absorption of $CuWO_4$ unravels the JT distortion and associated E_{JT} through the characteristic d-orbital splitting pattern of Cu^{2+} measured as a function of pressure up to 20 GPa. Pressure continuously reduces the JT distortion and E_{JT} of CuO_6 up to the triclinic-to-monoclinic phase transition at 9.9 GPa. Contrary to expectations, both the distortion and JT energy abruptly increase at the phase transition, which is a quite unconventional phenomenon. The reaction of CuO_6 octahedron against the reduction of the JT distortion suggests that the JT effect is the main driving force triggering the phase transition. The pressure-induced structural variations modify the exchange paths between Cu^{2+} ions yielding a change in the $CuWO_4$ magnetic behavior from antiferromagnetic to ferromagnetic as has been recently suggested from *ab initio* calculations [19]. Accordingly, the present results constitute experimental support for understanding the changes of magnetic properties through structural transformations mediated by the JT effect.

C.-Y. Tu is acknowledged for providing us the crystals used to perform the experiments. J. R.-F. is indebted to the FPI research grant (BES-2008-002043) and thanks C. Renero-Lecuna for fruitful discussions on the spectroscopic data. The authors thank the financial support from the MICINN of Spain under Grants No. MAT2010-21270-C04-01, No. MAT2008-06873-C02-01/02, and No. CSD2007-00045.

*Corresponding author.
javier.ruiz-fuertes@uv.es

[1] V. Z. Kresin and S. A. Wolf, Rev. Mod. Phys. **81**, 481 (2009).
[2] J. Bardeen, L. N. Cooper, and J. R. Schrieffer, Phys. Rev. **108**, 1175 (1957).
[3] C. W. Chu, P. H. Hor, R. L. Meng, L. Gao, Z. J. Huang, and Y. Q. Wang, Phys. Rev. Lett. **58**, 405 (1987).
[4] R. Griessen, Phys. Rev. B **36**, 5284 (1987).
[5] I. B. Bersuker, *The Jahn-Teller Effect* (Cambridge University Press, Cambridge, England, 2006).
[6] H. Keller, A. Bussmann-Holder, and A. Müller, Mater. Today **11**, 38 (2008).
[7] A. J. Millis, B. I. Shraiman, and R. Mueller, Phys. Rev. Lett. **77**, 175 (1996).
[8] I. Loa, P. Adler, A. Grzechnik K. Syassen, U. Schwarz, M. Hanfland, G. Kh. Rozenberg, P. Gorodetsky, and M. P. Pasternak, Phys. Rev. Lett. **87**, 125501 (2001).
[9] M. Baldini, V. V. Struzhkin, A. F. Goncharov, P. Postorino, and W. L. Mao, Phys. Rev. Lett. **106**, 066402 (2011).
[10] F. Rodríguez, in *High-Pressure Crystallography*, NATO Science for Peace and Security Series B (Springer, New York, 2010), pp. 215–229.
[11] F. Aguado, Ph.D. thesis, University of Cantabria, 2005.
[12] F. Aguado, F. Rodríguez, R. Valiente, M. Hanfland and J.-P. Itié, J. Phys. Condens. Matter **19**, 346229 (2007).
[13] J. Ruiz-Fuertes, A. Friedrich, J. Pellicer-Porres, D. Errandonea, A. Segura, W. Morgenroth, E. Haussühl, C.-Y. Tu, and A. Polian, Chem. Mater. **23**, 4220 (2011).
[14] V. Panchal, A. Segura, and J. Pellicer-Porres, High Press. Res. **31**, 445 (2011).
[15] A. Segura, J. A. Sans, D. Errandonea, D. Martínez-García, and V. Fages, Appl. Phys. Lett. **88**, 011910 (2006).
[16] F. Rodríguez, D. Hernández, J. García-Jaca, H. Ehrenberg, and H. Weitzel, Phys. Rev. B **61**, 16 497 (2000).
[17] R. Valiente and F. Rodriguez, Phys. Rev. B **60**, 9423 (1999).
[18] J. Ruiz-Fuertes, M. N. Sanz-Ortiz, J. González, F. Rodríguez, A. Segura, and D. Errandonea, J. Phys. Conf. Ser. **215**, 012048 (2010).
[19] J. Ruiz-Fuertes, D. Errandonea, R. Lacomba-Perales, A. Segura, J. González, F. Rodríguez, F. J. Manjón, S. Ray, P. Rodríguez-Hernández, A. Muñoz, Zh. Zhu, and C.-Y. Tu, Phys. Rev. B **81**, 224115 (2010).
[20] M. N. Sanz-Ortiz and F. Rodriguez, J. Chem. Phys. **131**, 124512 (2009).